Arrays of (Zn,Mn)S quantum wires with well-defined diameters below 10 nm ⊘

L. Chen; P. J. Klar; W. Heimbrodt; F. J. Brieler; M. Fröba; H.-A. Krug von Nidda; T. Kurz; A. Loidl
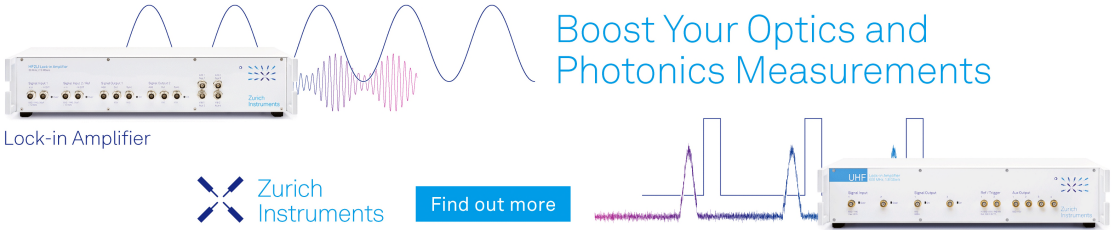
Check for updates

View Online

Export Citation

Arrays of (Zn,Mn)S quantum wires with well-defined diameters below 10 nm

L. Chen, P. J. Klar,[a] and W. Heimbrodt
Department of Physics and Material Sciences Center, Philipps-University Marburg, Renthof 5, 35032 Marburg, Germany

F. J. Brieler and M. Fröba[b]
Institute of Inorganic and Analytical Chemistry, Justus-Liebig University Giessen, Heinrich-Buff-Ring 58, 35392 Giessen, Germany

H.-A. Krug von Nidda, T. Kurz, and A. Loidl
Experimentalphysik V, EKM, Department of Physics, University of Augsburg, Universitätsstraße 2, 86135 Augsburg, Germany

$Zn_{1-x}Mn_xS$ with $x=1\%$ to 30% were formed inside the ordered pore systems of different mesoporous SiO_2 matrices. Due to the highly ordered host structure, regular arrays of $Zn_{1-x}Mn_xS$ quantum wires with diameters of 3.1 nm and 5.6 nm, respectively, separated by 2 nm SiO_2 barriers were obtained. The wires were characterized using photoluminescence (PL), PL excitation (PLE) spectroscopy, and electron paramagnetic resonance (EPR). The $^4T_1 \rightarrow {}^6A_1$ internal transition of the $Mn^{2+}(3d^5)$ ions dominates the PL. The corresponding PLE spectra show higher internal Mn transitions and the band-to-band transition. EPR spectra and the energies of the internal Mn transitions are typical for Mn^{2+} on a cation site of (II,Mn)VI semiconductors. The crystal field parameters indicate that the wires are tensilely strained. Due to the comparable band gaps of the SiO_2 and the $Zn_{1-x}Mn_xS$ and the small exciton Bohr radius in (Zn,Mn)S, the confinement effects in the wires are less than 150 meV.   © *2003 American Institute of Physics.*
[DOI: 10.1063/1.1530721]

09 April 2024 09:11:29

The organic-template directed synthesis of mesoporous silica in 1992 by Mobil Oil Company has led to a fast development of new synthesis pathways for materials with tailored porous structures. Depending on the synthesis conditions and the choice of organic template, highly ordered mesoporous SiO_2 superstructures can be prepared. Best known are the so-called M41S materials of hexagonal [(MCM-41) MCM: Mobil's composition of matter] and of cubic (MCM-48) symmetry with typical pore sizes ranging from 2 to 8 nm.[1,2] Recently, other organic structure directors based on block copolymers were developed, allowing one to vary the pore sizes over an even wider range up to about 30 nm.[3] The corresponding hexagonal mesoporous SiO_2 superstructures are referred to as SBA-15 structures (SBA: Santa Barbara). Removing the organic template of the three-dimensional superstructures in a calcination process leaves a highly ordered mesoporous SiO_2 matrix with regular wire-like pores of well-defined diameters. These mesoporous SiO_2 materials are ideally suited as host materials for semiconductors due to their high degree of order as well as the large band gap of the SiO_2 (which serves as barrier material). Several semiconductor compounds, e.g., CdS,[4] CdSe,[5] GaAs,[6] InP,[7] Ge,[8] SiGe,[9] (Cd,Mn)S,[10,11] or (Cd,Mn)Se[12] have been incorporated into MCM-41 SiO_2 matrices. Here, we demonstrate by incorporation of (Zn,Mn)S into SBA-15 SiO_2 matrices that high-quality semiconductor wire structures can be synthesized by incorporation into mesoporous SiO_2 matrices other than M41S.

Figure 1(a) shows a transmission electron microscopic image of a grain of hexagonal SBA-15 silica before incorporation of the semiconductor. The regular arrangement of the pores and the well-defined diameters are clearly visible. The latter is further confirmed by the pore size distributions [Fig. 1(b)] of (3.1 ± 0.1) nm and (5.6 ± 0.3) nm for the MCM-41 and SBA-15 silica matrices, respectively, determined by physisorption before incorporation.[13]

Figure 2 shows EPR spectra of five $Zn_{1-x}Mn_xS$ wire samples with diameters of 5.6 nm and with $x=1\%$, 5%, 10%, 20% and 30%, respectively. All spectra were taken at 4 K and normalized to the same amplitude. The EPR spectra are typical for exchange-coupled Mn^{2+} ions in (Cd,Mn) and (Zn,Mn) chalcogenide mixed crystals.[14–16] The EPR spectra consist of a sextet of sharp lines, each line with a pair of satellites at a lower magnetic field on a broad background. The sharp lines and their satellites correspond to the "allowed" ($\Delta m_S = \pm 1$ and $\Delta m_I = 0$) and the "forbidden" ($\Delta m_S = \pm 1$ and $\Delta m_I = \pm 1$) hyperfine transitions of the Zeeman-split $m_S = -1/2$ and $m_S = +1/2$ levels of the $^6S_{5/2}$ (or $^6A_1$) ground state of the Mn^{2+} $3d$ electrons. With increasing x, the structures are smeared out due to the increasing superexchange interaction between the Mn^{2+} ions.[17,18] The g factor is 1.999(2), close to 2.0 as expected for a pure S-state ion. A similar series of EPR spectra has been observed for other (II,Mn)VI wire structures.[11,12]

[a]Electronic mail: klarp@mailer.uni-marburg.de
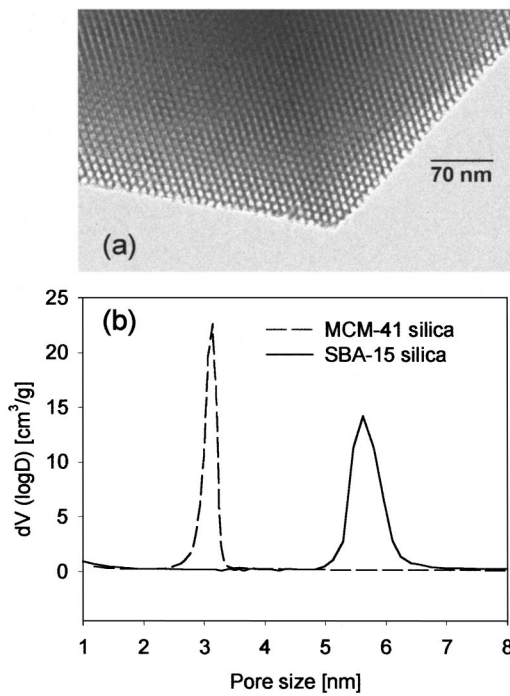[b]Electronic mail: michael.froeba@anorg.chemie.uni-giessen

FIG. 1. (a) High-resolution transmission electron microscopic image of the surface of a grain of the SBA-15 SiO_2 matrix material before incorporation of the semiconductor. (b) Pore size distribution of MCM-41 and SBA-15 mesoporous SiO_2 before incorporation determined by physisorption.
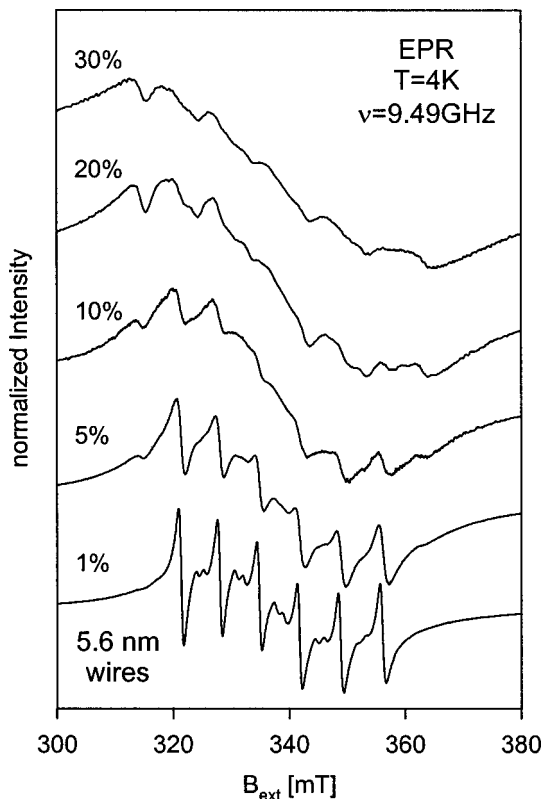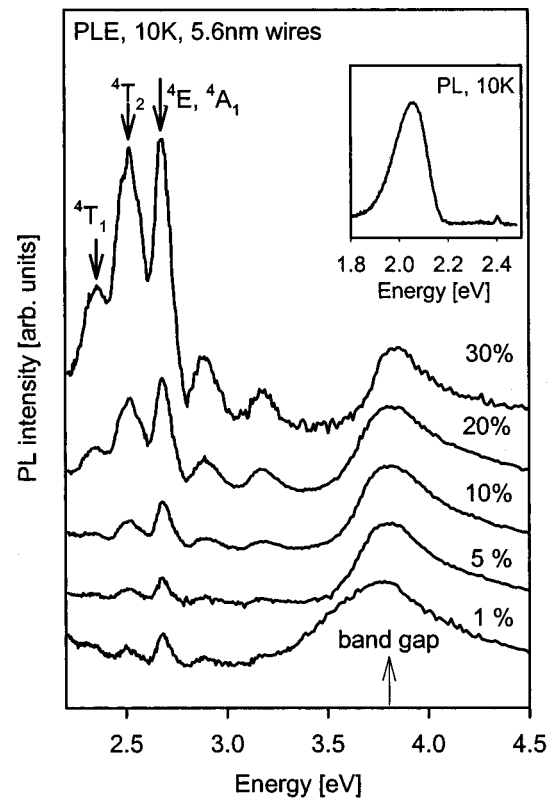

FIG. 3. PLE spectra of five $Zn_{1-x}Mn_xS$ in mesoporous SBA-15 SiO_2 samples of different Mn-content x. The PLE spectra were recorded at $T = 10$ K detecting the Mn-related PL (see inset).

Figure 3 depicts PLE spectra of the series of $Zn_{1-x}Mn_xS$ quantum wire samples with 5.6 nm diameter and x varying between 1% and 30% taken at 10 K. The PLE spectra were detected on the so-called yellow PL band (see inset of Fig. 3) originating from the $^4T_1$ to $^6A_1$ transition within the $3d^5$ shell of Mn^{2+}. This PL band is a common feature of wide-gap (II,Mn)VI compounds.[19–21] Because of the efficient energy transfer from the $Zn_{1-x}Mn_xS$ band states into the Mn^{2+}-subsystem, there is no band gap related excitonic PL observable. The PLE spectra show a distinct series of peaks. The broader band at the highest energies is the band-to-band transition of the wires. This signal is seen only because of the efficient energy transfer from the band states into Mn^{2+} $3d^5$ shell. The band gap shows quantum confinement, but only a weak dependence on Mn concentration. This is somehow expected as the band gaps of bulk ZnS and MnS are very similar, 3.78 eV and 3.7 eV, respectively.[22,23] The signals at lower energies are due to the direct absorption of the Mn^{2+} $3d^5$-shell and correspond to transitions from the $^6A_1$ ground state to the higher excited states $^4T_1$, $^4T_2$, and ^4E, $^4A_1$. This confirms that the Mn^{2+} ions are incorporated on Zn sites in the (Zn,Mn)S wires. The increase in intensity with respect to the band gap-related feature reflects the increase of the absorption due to the $3d$ shell of Mn^{2+} with increasing x. The transition energies of the Mn-internal transitions are approximately independent of x up to 30%. The PLE spectra of the 3.1 nm $Zn_{1-x}Mn_xS$ quantum wires are similar to those of the 5.6 nm samples, only the band gap-related signal is shifted to higher energies due to an increased quantum confinement.
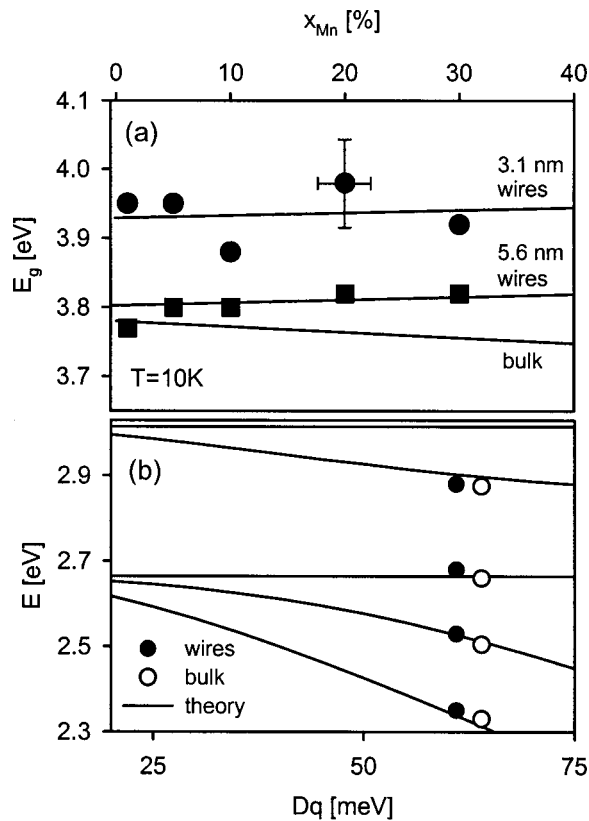

FIG. 2. Normalized EPR spectra of five $Zn_{1-x}Mn_xS$ in mesoporous SBA-15 SiO_2 samples of different Mn-content x at $T = 4$ K using the X-band frequency of 9.49 GHz.

FIG. 4. (a) Comparison of the band gap variation with x for $Zn_{1-x}Mn_xS$ wires of 3.1 nm and 5.6 nm at $T = 10$ K. The corresponding solid lines are guides for the eye. The lowest solid line represents the band gap change for bulk $Zn_{1-x}Mn_xS$ extrapolated from the band gaps of the binaries MnS and ZnS. (b) Energies of the internal transitions of Mn^{2+} ions in a T_d symmetric crystal field versus the field parameter Dq using the Racah parameters $B = 50$ meV and $C = 434$ meV, calculated in the framework of the Tanabe–Sugano model. Experimental points for $Zn_{0.9}Mn_{0.1}S$ bulk and wires.

Figure 4(a) depicts the variation of band gap with x for the $Zn_{1-x}Mn_xS$ wires of 3.1 and 5.6 nm extracted from the PLE spectra taken at 10 K. The solid line represents the band gap change for bulk $Zn_{1-x}Mn_xS$ and is derived by linear extrapolation between the values of the binaries.[22,23] It can be seen that confinement effects increase with decreasing wire diameter. For the 3.1 nm wires, the confinement energy is about 150 meV. This is smaller than the ~400 meV for (Cd,Mn)Se or 200 meV for (Cd,Mn)S wires of similar diameters.[12] This is expected as, going from (Cd,Mn)Se to (Cd,Mn)S to (Zn,Mn)S, the band gap difference (potential depth) between (II,Mn)VI and SiO_2, as well as the exciton Bohr radius, are decreasing.

Compared to bulk (Zn,Mn)S, the energies of the internal transitions are shifted by up to 30 meV to higher energies indicating a decrease of the crystal field around the Mn^{2+} site. In Fig. 4(b), the energies of the lowest excited states of a Mn^{2+} $3d^5$ ion in a T_d symmetric ligand field are depicted for a bulk $Zn_{0.9}Mn_{0.1}S$ sample (open circles) and the $Zn_{0.9}Mn_{0.1}S$ wires (full circles). The curves have been calculated in the Tanabe–Sugano model[24] as a function of the crystal field parameter Dq with the Racah parameters B

$= 50$ meV and $C = 434$ meV. The best fit yields $Dq = 0.61$ for the wires, which is somewhat smaller than the bulk value of $Dq = 0.64$. As Dq is indirectly proportional to the fifth power of the anion–cation distance this might be tentatively taken as a first indication for a tensile strain inside the pores.

We have demonstrated that high-quality (Zn,Mn)S can be incorporated into mesoporous silica matrices with well-defined, adjustable pore diameters. Such highly ordered mesoporous inorganic structures synthesized by organic-template directed pathways will offer possibilities for constructing regular magnetic semiconductor structures on length scales not accessible by standard lithography methods. Therefore, these growth techniques are of interest for applications as well as for fundamental studies of magnetic phenomena.

[1] C. T. Kresge, M. E. Leonowicz, W. J. Roth, J. C. Vartuli, and J. S. Beck, Nature (London) **359**, 710 (1992).

[2] Q. Huo, D. I. Margolese, U. Ciesla, P. Feng, T. E. Gier, P. Sieger, R. Leon, P. M. Petroff, F. Schüth, and G. D. Stucky, Nature (London) **368**, 317 (1994).

[3] D. Zhao, J. Feng, Q. Huo, N. Melosh, G. H. Fredrickson, B. F. Chmelka, and G. D. Stucky, Science **279**, 548 (1998).

[4] T. Hirai, H. Okubo, and I. Komasawa, J. Phys. Chem. B **103**, 4228 (1999).

[5] H. Parala, H. Winkler, M. Kolbe, A. Wohlfahrt, R. A. Fischer, R. Schmechel, and H. von Seggern, Adv. Mater. **12**, 1050 (2000).

[6] V. I. Srdanov, I. Alxneit, G. D. Stucky, C. M. Reaves, and S. P. DenBaars, J. Phys. Chem. B **102**, 3341 (1998).

[7] J. R. Agger, M. W. Anderson, M. E. Pemble, O. Terasaki, and Y. Nozue, J. Phys. Chem. B **102**, 3345 (1998).

[8] R. Leon, D. Margolese, G. Stucky, and P. M. Petroff, Phys. Rev. B **52**, R2285 (1995).

[9] Y. S. Tang, S. Cai, G. Jin, J. Duan, K. L. Wang, H. M. Soyez, and B. S. Dunn, Appl. Phys. Lett. **71**, 2449 (1997).

[10] L. Chen, P. J. Klar, W. Heimbrodt, F. Brieler, and M. Fröba, Appl. Phys. Lett. **76**, 3531 (2000).

[11] F. J. Brieler, M. Fröba, L. Chen, P. J. Klar, W. Heimbrodt, H.-A. Krug von Nidda, and A. Loidl, Chem. Eur. J. **8**, 185 (2002).

[12] L. Chen, H. Falk, P. J. Klar, W. Heimbrodt, F. Brieler, M. Fröba, H.-A. Krug von Nidda, A. Loidl, Z. Chen, and Y. Oka, Phys. Status Solidi B **229**, 31 (2002).

[13] M. Thommes, R. Köhn, and M. Fröba, J. Phys. Chem. B **104**, 7932 (2000).

[14] J. Schneider, S. R. Sircar, and A. Räuber, Z. Naturforsch. A **18**, 980 (1963).

[15] J. Lambe and C. Kikuchi, Phys. Rev. **119**, 1256 (1960).

[16] Y. Ishikawa, J. Phys. Soc. Jpn. **21**, 1473 (1966).

[17] N. Samarth and J. K. Furdyna, Phys. Rev. B **37**, 9227 (1988).

[18] O. Goede, D. Backs, W. Heimbrodt, and M. Kanis, Phys. Status Solidi B **151**, 311 (1989).

[19] O. Goede and W. Heimbrodt, Phys. Status Solidi B **146**, 11 (1988).

[20] O. Goede, W. Heimbrodt, and V. Weinhold, Phys. Status Solidi B **136**, K49 (1986).

[21] W. Heimbrodt, C. Benecke, O. Goede, and H.-E. Gumlich, Phys. Status Solidi B **154**, 405 (1989).

[22] D. Theis, Phys. Status Solidi B **79**, 125 (1967).

[23] O. Goede, W. Heimbrodt, M. Lamla, and V. Weinhold, Phys. Status Solidi B **146**, K65 (1989).

[24] Y. Tanabe and S. Sugano, J. Phys. Soc. Jpn. **9**, 753 (1954).